Materials Today Bio 29 (2024) 101274

Contents lists available at ScienceDirect

Materials Today Bio

journal homepage: www.journals.elsevier.com/materials-today-bio

All-organic transistors printed on a biodegradable and bioderived substrate for sustainable bioelectronics

Fabrizio A. Viola [a,b,1,*], Ksenija Maksimovic [a,1], Pietro Cataldi [c], Camilla Rinaldi [c,d], Elena Stucchi [a,e], Filippo Melloni [a,e], Athanassia Athanassiou [c], Mario Caironi [a,**]

[a] Center for Nano Science and Technology, Istituto Italiano di Tecnologia, Via Rubattino 81, 20134, Milan, Italy
[b] Department of Electrical and Electronic Engineering, Università degli Studi di Cagliari, Via Marengo 3, 09123, Cagliari, Italy
[c] Smart Materials, Istituto Italiano di Tecnologia, Via Morego 30, 16163, Genova, Italy
[d] Department of Earth and Environmental Science (DISAT), University of Milano-Bicocca, Piazza della Scienza, 20126, Milano, Italy
[e] Department of Physics, Politecnico di Milano, Piazza Leonardo da Vinci 32, 20133, Milano, Italy

ARTICLE INFO

Keywords:
Sustainable bioelectronics
Printed bioelectronics
Biopolymers
Biodegradable electronics
Biomaterials

ABSTRACT

Biodegradable electronics is an incipient need in order to mitigate the alarming increase of electronic waste worldwide caused by capillary penetration of electronic devices and sensors. Flexibility, solution processability, low capital expenditure, and energy-efficient processes, which are distinctive features of organic printed electronics, have to be complemented by a sustainable sourcing and end-of-life of materials employed. This requirement calls for solutions where materials, especially substrates that typically represent the largest volume, can be biodegraded in the environment with no harm, yet assuring that no precious resources are dispersed. In this work, the bioderived and biodegradable biopolymer polyhydroxybutyrate (PHB) was used as a substrate, cast from an acetic acid solution, for all-organic field effect transistors (OFETs) based on an inkjet printed polymer semiconductor. The OFETs showed small device-to-device variation, a proper current modulation with I_{ON}/I_{OFF} of about $1.2{\cdot}10^3$, mobility values as high as 0.07 cm^2/Vs in saturation regime and channel length/width normalized leakage currents in the order of nA, which remained almost unaltered also after intensive mechanical stresses upon bending and rolling. Such mechanical stability and flexibility, together with the biodegradability and bioderivation, make PHB an appealing candidate for the development of sustainable printed bioelectronics, with widespread future applications in the biomedical and food packaging sector.

1. Introduction

The continuous advancements in the field of electronics, together with a rapid reduction of its costs, allowed the development of smart household appliances as well as powerful and numerous portable devices, which are easily accessible to an ever larger portion of the population. On the one hand, this has an undoubtedly positive effect on the society in terms of the quality of life and access to information. On the other, it is causing a continuous increase in the so-called electronic waste (e-waste), which is defined as anything with an electric cord, plug or battery (such as smartphones, televisions, computers, microwave ovens etc.) that have reached the end of their life [1]. According to "The Global E-Waste Monitor 2024" the amount of e-waste produced globally in 2022 reached a record of 62 million tonnes, which corresponds to about 7.8 kg produced yearly per person. The same report predicts that the global e-waste is expected to reach 82 million tonnes by 2030 [2]. One of the main issues related to e-waste is its improper disposal [3]. For this reason, in the last decade, both academic and industrial research put a lot of effort into the development of new technologies that are able to overcome and alleviate end-of-life issues. In particular, the emerging field of Internet-of-Things (IoT) can represent a further environmental hazard if counter measures are not considered in the design of future devices. Organic large-area and printed electronics is proposed as a strong candidate for more sustainable distributed electronics applications [4,5]. In fact, it is based on carbon materials, and can be produced with energy-efficient and cost-effective processes such as printing [6–9].

* Corresponding author. Department of Electrical and Electronic Engineering, Università degli Studi di Cagliari, Via Marengo 3, 09123, Cagliari, Italy.
** Corresponding author. Center for Nano Science and Technology, Istituto Italiano di Tecnologia, Via Rubattino 81, 20134, Milan, Italy.
E-mail addresses: fabrizioa.viola@unica.it (F.A. Viola), mario.caironi@iit.it (M. Caironi).
[1] Equally contributing first authors.

https://doi.org/10.1016/j.mtbio.2024.101274
Received 1 July 2024; Received in revised form 23 September 2024; Accepted 25 September 2024
Available online 26 September 2024

Nevertheless, typical plastic electronics does not yet meet necessary requirements on the biodegradability of adopted materials and on the necessity to avoid dispersion of resources.

In this scenario, since the substrate constitutes by far the largest fraction of the total weight of materials used for each device, the overall biodegradability properties are dominated by it. Therefore, ensuring biodegradability of the substrate, while preserving chemical, mechanical, and functional compatibility with the printed organic devices, is an effective strategy to drastically reduce the environmental impact of future large-area printed electronics [10].

To date, in literature several natural biodegradable materials have been used and reported to this purpose. Cellulose [11–13], silk [14–16], shellac [17–19], have been extensively studied and employed as substrates in many electronic applications, due to their excellent mechanical properties and flexibility.

Other natural polymers as gelatin [20], collagen [21], agarose [22], chitosan [23], and chitin [24] have been successfully used as green substrates.

On the one hand, all these natural-based materials bring together several advantages such as easy processability, low costs and abundant resources. On the other, severe limitations such as the lack of compatibility with various classes of organic solvents and with processes including even mild temperatures (i.e., above 80 °C), have largely precluded and still limit their employment and diffusion in electronic devices [10].

Bioplastics (i.e., a plastic material that is either biodegradable, biobased or both biobased and biodegradable [25,26]) can overcome such drawbacks and have been recently proposed as a biodegradable alternative for green electronics [27–31]. Among them, one of the most promising bioplastic is polyhydroxybutyrate (PHB). Indeed, it is the best-known biopolymer in the group of polyhydroxyalkanoates (PHAs), which are produced by different types of bacteria as an intercellular energy reserve and can be degraded by enzymes known as PHB-depolymerases, resulting in non-toxic products [32]. PHB biodegradability has been proven not only in composting plants, but also in free environments, such as soil and marine water, making it a more environmentally-friendly option with respect to other bio-based but not biodegradable bioplastics, such as poly(lactic acid) (PLA) [33–35]. Other advantages of PHB lie in its relatively high melting point (between 172 and 183 °C), well above that of natural materials such as shellac (~75 °C) and that of other bioplastics such as Mater-Bi (~70 °C), and in its non-toxicity and biocompatibility [36,37]. Moreover, its mechanical properties are similar to those of the well-known synthetic polypropylene (PP) [36], thus making PHB a suitable alternative to substitute PP in a wide range of applications.

In this work we have tested the use of PHB as a sustainable and flexible substrate for fully organic field-effect transistors (OFETs) based on printed polymers. PHB substrates were obtained by dissolving PHB pellets in the acetic acid solution, an alternative with a lower ecological hazard potential with respect to the commonly used chloroform, according to the Ecological Risk Classification of Organic Substances Approach (ERC). OFETs were fabricated on top by means of large-area and scalable fabrication techniques, such as inkjet-printing and chemical vapour deposition. During the device fabrication process, PHB could well withstand the maximum processing temperature of 120 °C, and the use of water, ethylene glycol, isopropanol and mesitylene solvents. The fully organic transistors showed small device-to-device variation, a particularly challenging feature to achieve when biodegradable substrates are employed, and a proper current modulation, having an I_{ON}/I_{OFF} of about $1.2{\cdot}10^3$, and a very low channel length/width normalized leakage currents, in the order of nA. Moreover, thanks to the superior thermal stability of PHB substrate, allowing the adoption of an optimal processing temperature as high as 120 °C, the proposed transistors showed a maximum charge carriers mobility of 0.07 cm^2/Vs, which is more than six times higher than what it has been previously reported for P(NDI2OD-T2) based OFETs printed on top of Mater-Bi biodegradable substrates [38]. Additionally, thanks to the mechanical properties of the PHB substrate, correct OFETs operation can be maintained also after intensive mechanical stresses such as bending and rolling, with mild effects on the electrical performance.

Such results provide a promising demonstration of the suitability of PHB for sustainable printed organic bioelectronics and can pave the way for the employment of new organic devices for applications, such as biomedical devices and food packaging, in which biodegradability together with intensive handling and mechanical robustness are required.

2. Materials and methods

2.1. Substrate preparation and deposition

Polyhydroxybutyrate (PHB) was purchased from Goodfellow in form of 5 mm nominal granule size. To prepare the films, it was dissolved in glacial acetic acid, purchased from Merck Millipore.

A solution of 0.05 g/mL of PHB in Acetic Acid was heated at 140 °C for about 40 min under constant stirring. About 1 mL of solution was drop-cast on a glass substrate (30 mm × 70 mm): both the solution and the glass substrate were previously heated at 120 °C to avoid thermal gradients. The deposition and the solvent evaporation were carried out under the fume hood where the films were kept until the complete solvent evaporation. The peeling-off of the solidified films from the glass substrate was done initially with tweezers and, once the detached surface was large enough, the process was ended by hand since the films were strong enough.

2.2. OFETs fabrication

All-organic n-type bottom-contact/top-gate field effect transistors were produced on top of the dried PHB films still attached to the glass substrate for the ease of handling. For the source and drain contacts, poly(3,4-ethylenedioxithiophene):polystyrene sulphonate (PEDOT:PSS) (Clevios PJ700 formulation, purchased from Heraeus), was inkjet-printed with a Fujifilm Dimatix DMP2831 through a cartridge with 10 pL nozzles and annealed at 120 °C for about 1 h in air. This technique allowed to produce transistors having channel length and width of about 60 μm and 800 μm, respectively. Source and Drain were printed at a drop spacing of 45 μm (one layer), a firing voltage of 40 V, a jetting frequency of 1 kHz, and the printer plate temperature was set to 28 °C.

On top of the contacts, a polyethylenimine (PEI)-based injection layer was printed. The solution was composed at 20 vol% by ethylene glycol, purchased form Sigma Aldrich, at 30 vol% of zinc oxide (ZnO) nanoparticles in isopropanol (nanoparticle concentration 2.5 wt%), and at 50 vol% of PEI branched polymer having Mw ≈ 10 000, purchased from Sigma Aldrich, and dissolved in water at 0.2 wt%. After the deposition, the PEI solution underwent annealing in air at 110 °C for 30 min. The n-type semiconductor, poly[N,N′-bis(2-octyldodecyl)-naphthalene-1,4,5,8- bis(dicarboximide) - 2,6-diyl]-alt-5,59-(2,29-bithiophene), P(NDI2OD-T2), was inkjet-printed from a mesitylene-based solution, with a concentration of 7 mg/mL and then annealed in nitrogen atmosphere for 3 h at 120 °C. It has been printed through a cartridge with 10 pL nozzles, at a drop spacing of 50 μm (one layer), a firing voltage of 35 V, and a jetting frequency of 1 kHz and the printer plate temperature was set to 28 °C. The dielectric used was a 250 nm thick Parylene-C layer purchased in dimer form from Specialty Coating Systems. It was chemically vapour deposited using a SCS Labcoater 2-PDS2010 system. The dimer was pyrolyzed at 690 °C and deposited at the ambient temperature between 8 and 10 mbar pressure. Finally, PEDOT:PSS gate contacts were inkjet printed on top of the dielectric layer and dried in vacuum for 10 min. Gate contacts were printed at a drop spacing of 40 μm (one layer), a firing voltage of 40 V, a jetting frequency of 1 kHz, and the printer plate temperature was set to 28 °C."

2.3. Electrical characterization

The devices were characterised by measuring the output and transfer curves with an Agilent B1500 A Semiconductor Parameter Analyzer in a glovebox under controlled nitrogen atmosphere. In order to measure the device functioning once the PHB films were detached from the glass substrate, the films were fixed again to the glass substrate with some tape to ensure the ease of handling. Linear and saturation regime transfer curves were measured at fixed drain voltages (V_{DS}) of 5 V and 20 V, respectively, for the gate voltage (V_{GS}) ranging from 0 V to 30 V, even though the transistors' proper functioning occurred already at less than 10 V. The output curves were measured for V_{DS} ranging from 0 V to 20 V at fixed V_{GS} spanning from 0 V to 20 V at steps of 4 V.

Parylene-C capacitance was extracted using an Agilent 4294A Impedance Analyzer with a two probes configuration, at a frequency of 40 Hz.

2.4. Mechanical characterization

PHB films' tensile properties were analyzed using uniaxial tensile tests in an INSTRON 3365 dynamometer equipped with a 2 kN load cell. ISO 527-1 was followed to perform the stress-strain measurements. The samples were cut to a dog-bone shape (Fig. S7 – Supporting Information), and a digital micrometer (Mitutoyo, accuracy 0.001 mm) was used to measure their thickness. The strain rate during the experiment was set at 5 mm min^{-1}. Seven specimens were analyzed, and their Young's modulus (MPa), tensile stress at break (MPa), and elongation at break (%) were extracted (see Table T1 – Supporting Information).

2.5. PHB surface characterization

2.5.1. Scanning electron microscope (SEM)

The morphology of the obtained material was analyzed by SEM, using a variable-pressure JEOL JSM -649LA (JEOL, Tokyo, Japan) microscope equipped with a tungsten thermionic electron source and working in high vacuum mode, with an acceleration voltage of 5 kV. The sample was coated with a 10 nm-thick film of gold utilizing the Cressington 208HR Sputter Coater (Cressington, Watford, UK).

2.5.2. Atomic force microscope (AFM)

An AFM system XE-100 (Park Scientific, Suwon, South Korea) with an NCHR probe (f = 320 kHz, c = 42 N/m) was used to investigate the topography of materials. Areas of 45 × 45 μm (2304 x 2304 pizels) and 5 × 5 μm (256 × 256 pixels) were scanned. The images were acquired in non-contact mode and then processed by Gwyddion software.

2.6. Biodegradability test

The biodegradability of the samples was tested following ISO 23977–2:2020, which standardizes how to measure the biochemical oxygen demand (BOD) in seawater over 30 days. Tested samples were the pure PHB substrate, PHB with OFETs printed on top, and polylactic acid biopolymer (PLA, grade 2003D purchased from NatureWorks) for comparison. Each sample was cut into small pieces, and about 140 mg of material was added to 432 mL of seawater from Porto Antico of Genoa. The experiment was performed at room temperature within autoclaved amber glass bottles with 510 mL volume. The BOD test operates on the principle that microorganisms consume oxygen while decomposing organic substances present within the water. Thus, the bottles were filled with seawater and hermetically closed with the OxiTop® OC 100 measuring heads. Sodium hydroxide tablets were used to sequester carbon dioxide produced during biodegradation. The biotic consumption of the oxygen present in the free volume of the system was measured as a function of the decrease in pressure. The mean values of the blanks obtained by measuring the seawater's oxygen consumption without any test material were subtracted from the raw oxygen consumption data (mg O_2/L). Then, values were normalized on the mass of the individual samples and referred to 100 mg of material (mg O_2/100 mg material). The BOD is calculated as the difference between the initial and final dissolved oxygen concentrations expressed as milligrams of oxygen per liter (mg/L) of water.

3. Results and discussion

The PHB film was fabricated by means of low-cost drop-casting technique, which consists of dissolving the polymer in an appropriate solvent, dropping it on a clean surface and waiting for the solvent evaporation, leaving behind a polymeric film. The main advantage of this technique is the possibility to finely tune the film properties by changing the solvent and process parameters such as the solution concentration, the casting temperature, and the casting time.

Chloroform is one of the most compatible and thus the most widely used solvent for PHB dissolution [39], nevertheless it is highly toxic both for humans and the environment and has been declared as potentially carcinogenic [40]. In the view of developing a biodegradable, environmental-friendly device, which can be potentially employed for biomedical or food-packaging applications, less harmful solvents were considered for PHB dissolution in order to reduce any issue related to solvent residuals. For that reason, acetic acid has been chosen since it has a lower hazard potential with respect to chloroform, according to the ERC, and it has already been employed with great success for the PHB dissolution [39]. After extensive testing of the drop-casting temperature from an acetic acid solution (see Supporting Information - section 1), the range between 100 °C and 120 °C was considered suitable for the formation of PHB films acting as substrates for OFETs fabrication (Fig. 1(a) and (b)), with a measured thickness of about 20 μm. The mechanical properties of the PHB substrates were evaluated by tensile testing, and the resulting stress-strain curves are shown in Supporting Information, Fig. S7 and Table T1. The surface characterization of the PHB substrates was evaluated by atomic force microscopy and scanning electron microscopy, and are shown in Supporting Information, Figure S8 and Figure S9. Interestingly, the obtained mechanical properties align with other works in literature that employ drop-cast polyhydroxyalkanoate biopolymers from acetic acid solutions and are comparable to similar films obtained using more toxic solvents such as chloroform [39].

Prior to the device fabrication, thermal and solvent resistance of PHB films were assessed to ensure their integrity during the entire production process. Upon a simple optical survey, films did not show evident effects upon application of temperatures up to 120 °C for 3 h and following dipping in water, ethylene glycol, isopropanol and mesitylene solvents.

The schematic representation of the produced OFETs, together with the chemical formulas of each layer of the structure is shown in Fig. 1 (c). The architecture employed is the staggered bottom-contact top-gate (BCTG) one, since it is characterized by a better charge injection and thus by a better performance with respect to the coplanar architecture [41].

Poly(3,4-ethylenedioxithiophene):polystyrene sulphonate (PEDOT:PSS) based source and drain contacts were inkjet printed on the PHB substrate and then annealed at 120 °C for 1 h in air, obtaining channels with a length of 60 μm and width of 800 μm. On top of them, a polyethylenimine (PEI)-based injection layer was inkjet printed in order to improve electrons injection into semiconductors for n-type operation [42–44]. Subsequently, the model n-type poly[N,N′-bis(2-octyldodecyl)-naphthalene-1,4,5,8-bis(dicarboximide)-2,6-diyl]-alt-5,59-(2,29-bithiophene) P(NDI2OD-T2) was inkjet printed as active layer and annealed at 120 °C for 3 h under nitrogen atmosphere. A Parylene-C dielectric layer, 250 nm thick, was deposited on all the substrate, resulting a capacitance around 10 nF/cm^2, as reported elsewhere [38]. As the final step, a PEDOT:PSS gate electrode was inkjet printed on top of each OFET and dried in vacuum to ensure solvent evaporation.

In order to evaluate the proper operation of the devices, as well as the

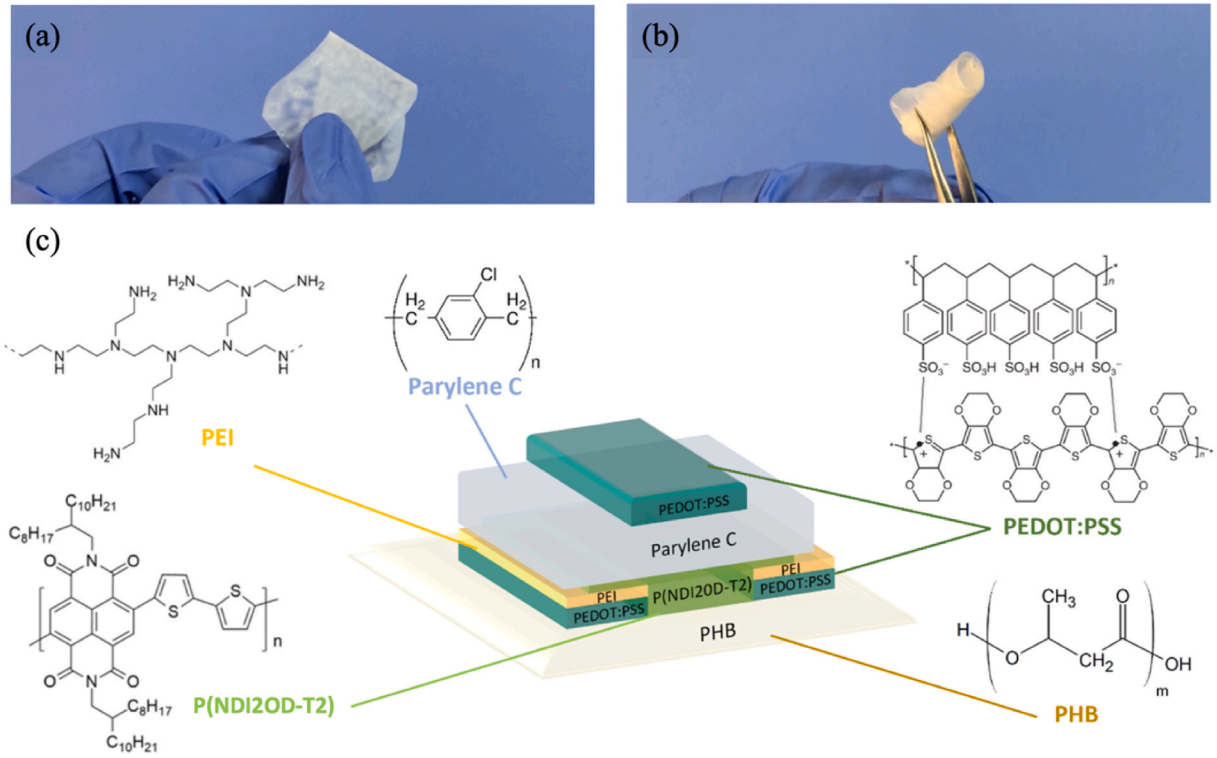

Fig. 1. Photographs of the PHB film used as device substrate when (a) bended and (b) rolled. (c) Schematic representation of the structure of the produced all-organic OFETs and chemical formulas of the polymers employed.

reproducibility of the process, the first electrical characterization was performed while the films were still attached on the glass substrate: 8 identical OFETs were electrically analyzed, and their average properties were extracted and reported in Table 1. From the characteristic transfer curves in linear regime (at $V_{DS} = 5$ V) and saturation regime (at $V_{DS} = 20$ V), shown in Fig. 2 (a) for a single device, and in Fig. 2 (b) for all 8 devices (raw data are reported in Supporting Information – section 3), a proper n-type current modulation can be appreciated, with an average maximum source-drain current (I_{DS}) of (0.63 ± 0.16) μA, in linear, and of (3.12 ± 0.42) μA, in saturation regime (at $V_{GS} = 30$ V). The limited I_{DS} standard deviation, evaluated on 8 devices, corresponds to 25 % and 13 % of the mean value in linear and saturation regime respectively, indicates a very small device-to-device variation.

The current on/off ratio (I_{ON}/I_{OFF}), defined as the ratio between the maximum current achieved in the on-state and the minimum one in the off-state of the device in the explored voltage window, is above 10^3, for both linear and saturation regime. The threshold voltage, V_{TH}, is (4 ± 1.5) V in linear and (3.2 ± 0.8) V in saturation regime. For the proposed OFETs the sub-threshold swing (*SS*) amounts to (2.6 ± 0.8) V/dec. From the shape of transfer curves for a single device (Fig. 2 (a)), a very slight hysteresis can be observed: during the backward sweep the curve presents a slight shift toward negative voltages.

In Fig. 2 (c), the corresponding output curves of one device are reported. The initial part of the curves deviates from the ideal linearity in a slightly "S" shaped form, indicating the presence of a contact resistance caused by non-ideal contacts [45,46]. The contact resistance, extracted by using the Y-function method in linear regime, has a value of $R_C \times W = (2.7 \pm 1.3)*10^6$ Ω cm. Nevertheless, the effect does not preclude the correct device functioning.

Apparent linear ($\mu_{lin,app}$) and saturation ($\mu_{sat,app}$) field-effect mobilities were calculated using equations derived under the assumption of the gradual channel approximation [47]. The average mobility curves of 8 devices are shown in Fig. 2 (d). The maximum mobility values of (0.04 ± 0.006) cm^2/Vs and of (0.07 ± 0.009) cm^2/Vs, respectively for linear and saturation regime, were calculated according to Choi et al. [48], with a reliability factor (*r*) of 0.83 ± 0.06 for the linear (r_{lin}) and 0.72 ± 0.03 for the saturation (r_{sat}) regime. It is worth noting that the limited standard deviation of transfer characteristic curves (Fig. 2 (b)) and consequently of the main electrical parameters (Table 1), indicate a small device-to-device variation of OFETs directly patterned on the prepared PHB substrate.

Such solid estimation indicates that the mobility achieved with the proposed transistors is in line with what has been consistently reported for conventional low-voltage, printed, P(NDI2OD-T2)-based OFETs where the Parylene-C dielectric is directly deposited onto the organic semiconductor without any interlayer [49]. Moreover, when comparing

Table 1
Average parameters of all-organic OFETs printed on the PHB as fabricated, after the detachment from a glass substrate and after the rolling stress.

	As fabricated (on glass carrier)		After detachment		After rolling	
	Linear regime	Saturation regime	Linear regime	Saturation regime	Linear regime	Saturation regime
I_{ON}/I_{OFF}	(1.7 ± 0.7) ·10^3	(1.2 ± 0.5) ·10^3	(1.3 ± 0.5) ·10^3	(1.3 ± 0.5) ·10^3	(3.5 ± 2.1) ·10^3	(2.5 ± 1.1) ·10^3
V_{TH} *[V]*	4 ± 1.5	3.2 ± 0.8	3 ± 0.9	2.8 ± 0.2	4.5 ± 1	3.6 ± 0.6
SS *[V/dec]*	2.6 ± 0.8	/	2.3 ± 0.6	/	1.9 ± 0.2	/
Normalized I_{GS} max *[A]*	1.1 ·10^{-8}	6.4 ·10^{-9}	9 ·10^{-9}	5.1 ·10^{-9}	4.1 ·10^{-8}	3 ·10^{-8}
μ_{app} *[cm^2/Vs]*	0.04 ± 0.006	0.07 ± 0.009	0.03 ± 0.006	0.05 ± 0.006	0.02 ± 0.006	0.04 ± 0.008
r factor	0.83 ± 0.06	0.72 ± 0.03	0.86 ± 0.04	0.74 ± 0.05	0.78 ± 0.06	0.72 ± 0.01

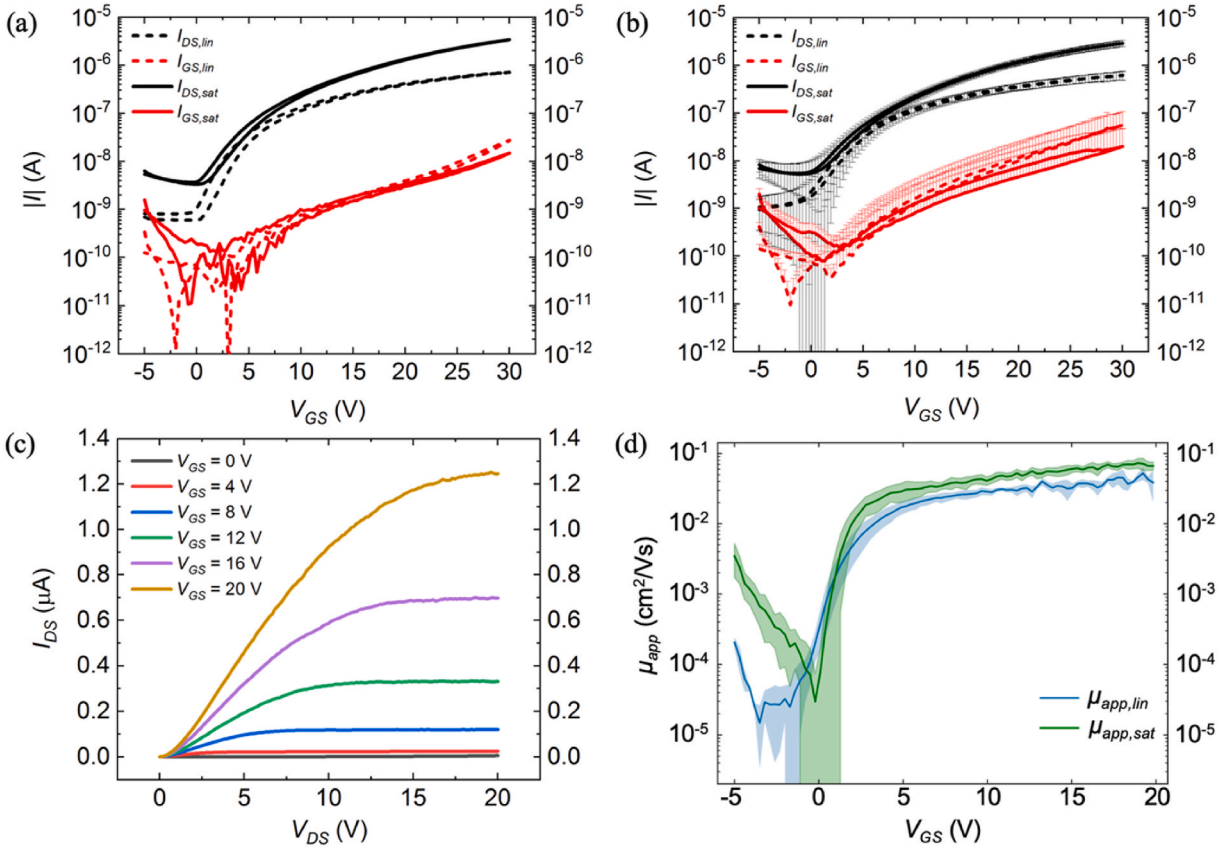

Fig. 2. Transfer curves in linear (V_{DS} = 5 V) and saturation (V_{DS} = 20 V) regimes together with their leakage gate currents, I_{GS}, of (a) a single device and (b) of the average of 8 devices (for I_{GS} only the upper part of the confidence band is shown for clarity). (c) Output curves of a single OFET for V_{GS} ranging from 0 V to 20 V at steps of 4 V. (d) Linear ($\mu_{lin,app}$) and saturation ($\mu_{sat,app}$) apparent mobility plots with their standard deviations of 8 devices.

the proposed devices with what has been reported for printed P(NDI2OD-T2)-based OFETs on top of biodegradable Mater-Bi substrate, the mobility achieved here is more than six times higher, due to the higher thermal stability of PHB substrate with respect to Mater-Bi, and therefore the possibility to apply optimized thermal annealing steps during the fabrication process [38]. Furthermore, to facilitate comparison between our devices and the non-biodegradable n-type OFETs reported in the literature, we provide the relevant performance

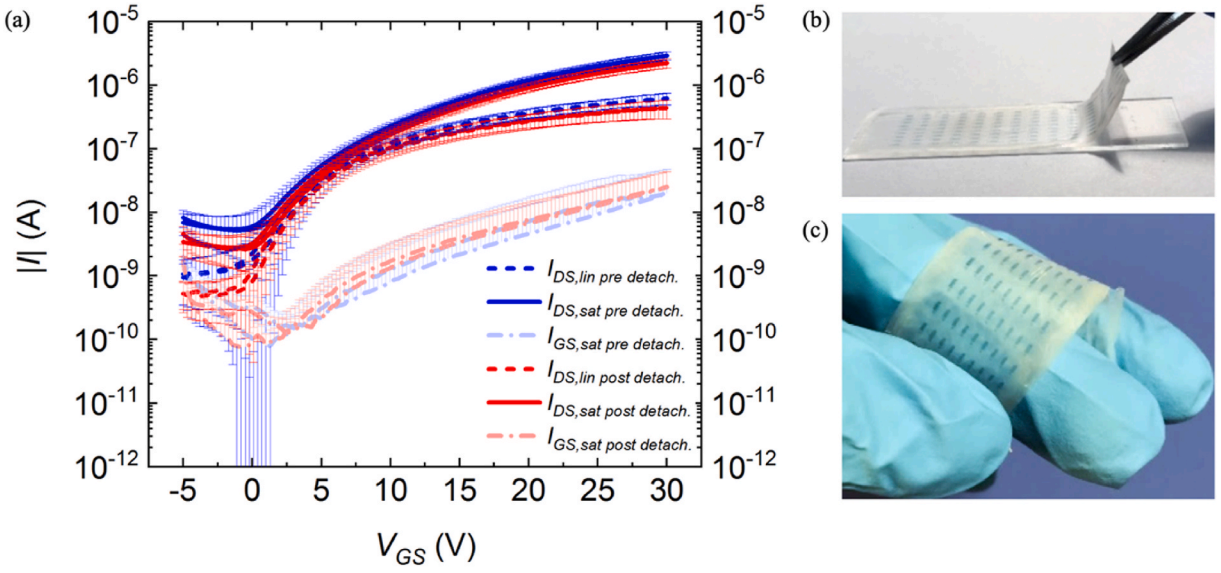

Fig. 3. (a) Characteristic linear (dashed lines) and saturation (full lines) regime transfer and leakage current curves (dot-dashed lines) of many OFETs produced on a PHB film before (blue) and after (red) its detachment from the glass substrate. Photographs (b) of the detachment process of the PHB film, carrying on top all-organic OFETs, from the glass substrate and (c) of the final result: self-standing and flexible OFETs on the PHB substrate. (For interpretation of the references to colour in this figure legend, the reader is referred to the Web version of this article.)

data of state-of-the-art devices in the Supporting Information (Table T2).

After having evaluated the proper operation and the electrical performance of the proposed devices as fabricated on the glass carrier, the PHB substrate with OFETs has been mechanically detached.

The detachment, shown in Fig. 3 (b), did not lead to any evident or visible mechanical deformation or rupture of the structure. After detachment, 8 OFETs were measured and their properties compared to those obtained with the same devices before detachment (see Table 1, while the raw data are reported in Supporting Information – section 3). As it can be seen in Fig. 3 (a), the transfer curves of the detached devices (red) are just slightly lower than those of the first characterization (blue), following a shift towards more negative values of $V_{TH,lin}$ (from 4 ± 1.5 V to 3 ± 0.9 V) and $V_{TH,sat}$ (from 3.2 ± 0.8 V to 2.8 ± 0.2 V). Indeed, the I_{ON}/I_{OFF} remained almost unaltered, as well as the subthreshold swing. As for the apparent mobility, it was reduced from (0.04 ± 0.006) cm^2/Vs to (0.03 ± 0.006) cm^2/Vs in the linear regime, and from (0.07 ± 0.009) cm^2/Vs to (0.05 ± 0.006) cm^2/Vs in the saturation regime, while the reliability factors resulted to be in line with the previous analysis. Moreover, as reported in Table 1, no significant variations were recorded in the average leakage current (I_{GS}), which remained unchanged in both the linear and saturation regimes.

To assess the mechanical stability under bending stress, the same electrical characterization was performed on 5 OFETs after having rolled the film at a bending radius of 2.5 mm (which corresponds to a surface strain of 0.4 %), as shown in Fig. 4 (b). The average transfer curves of this further measurement were superimposed to the curves acquired for the devices on glass, as represented in Fig. 4 (a), and their parameters were calculated and reported in Table 1 (the raw data are reported in Supporting Information – section 3). In this case some weak but more evident effect on the transfer curves is visible, due to the mechanical stress applied on the active area of the transistor [50], with lower maximum drain currents of (0.38 ± 0.1) μA and (2.01 ± 0.4) μA, respectively in linear and saturation regime, and comparable I_{ON}/I_{OFF}. The more evident changes in parameters after rolling can be ascribed to the harsher mechanical stress undergone by the devices. The modest changes suggest that further optimizations, including for example the use of neutral plane configuration, are highly promising towards obtaining very robust printed circuits on PHB. As reported in Table 1, the maximum leakage currents increased for both regimes, specifically from 120 nA to 530 nA in linear and from 68 nA to 400 nA, while the V_{TH} shifted toward more positive values (from 3 ± 0.9 V to 4.5 ± 1 V in linear regime, and from 2.8 ± 0.2 V to 3.6 ± 0.6 V in saturation regime). The mobility experienced a decrease, reaching values of (0.02 ± 0.006) cm^2/Vs for $\mu_{lin,app}$ having a r_{lin} of 0.78 ± 0.06, and of (0.04 ± 0.008) cm^2/Vs for $\mu_{sat,app}$ with r_{lin} of 0.72 ± 0.01.

Neither the delamination, nor the rolling stress hampered the proper functioning of the device, offering a promising evidence for use of PHB and organic electronics for mechanically challenging applications. The small standard deviation of transfer curves measured both after detaching from the glass support (Fig. 3 (a)) and rolling the substrate (Fig. 4 (a)) are once again indicative of the small device-to-device variation and of the reliability of the process.

As already stated in the previous sections, the development of sustainable and biodegradable transistors may be instrumental for the widespread adoption of environmental monitoring systems that perform their function and do not need recollection after usage. Toward such an ambitious goal, we tested the biochemical oxygen demand (BOD) in seawater (according to the standard ISO 23977–2:2020), of the proposed OFETs printed on PHB.

BOD operates on the principle that microorganisms consume oxygen while decomposing organic substances present within the water. This medium typically shows slower degradation than soil for standard biopolymers [51]. Results are reported in Fig. 5: the devices printed on PHB are compared with the pure PHB substrates and PLA, one of the most widely employed commercially available biopolyesters. PLA did not start any biodegradation throughout the 30-day duration of the test, as expected [33,52]. In contrast, pristine and printed PHB substrate started their degradation between the 10th and 15th day, reaching BOD values of *ca.* 3 and 2 mg O_2/100 mg at the test end, respectively. The diverse degradation rate with and without the OFETs printed on the PHB substrates is due to the composition of the OFET materials, which are not easily digestible by microorganisms in the seawater. Such results are in line with similar devices printed on other biopolymers [38].

4. Conclusions

We proposed biodegradable and bioderived PHB substrates for large-area and printed electronics with sustainable life-cycle. PHB films were formed by drop-casting from an acetic acid solution, which is a lower environmental hazard alternative compared to the commonly used chloroform. All-organic FETs were successfully fabricated on top, by means of industrially viable, large-area techniques, such as inkjet

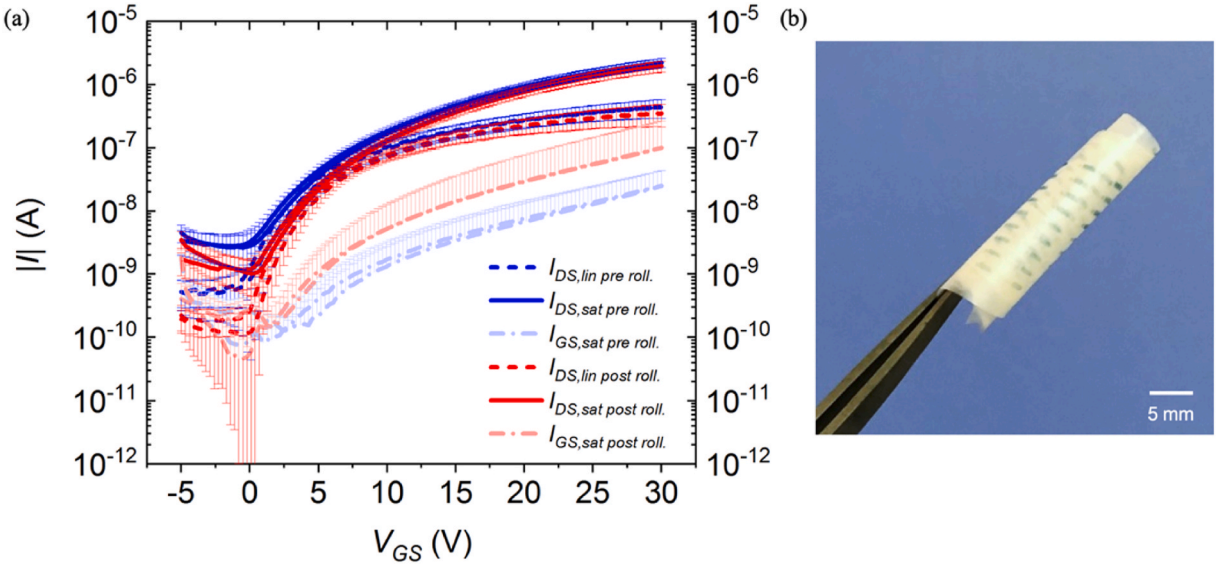

Fig. 4. (a) Characteristic linear (dashed lines) and saturation (full lines) regime transfer and leakage current curves (dot-dashed lines) of 5 OFETs produced on a PHB film before (blue) and after (red) its detachment from the glass substrate and after its rolling. (b) Photograph of the rolled PHB film with on top the all-organic OFETs. (For interpretation of the references to colour in this figure legend, the reader is referred to the Web version of this article.)

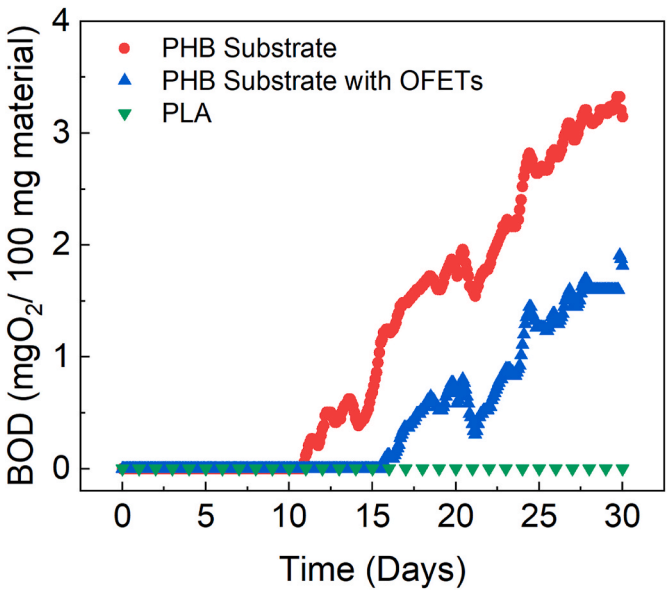

Fig. 5. Biochemical Oxygen Demand of the OFETs deposited on PHB substrates. PLA biopolymer is used for comparison.

printing for the PEDOT:PSS electrodes and the model P(NDI2OD-T2) semiconductor, and chemical vapour deposition for the Parylene-C dielectric. A maximum field-effect carrier mobility of 0.07 cm^2/Vs in saturation was achieved, exceeding what was previously reported for P(NDI2OD-T2) based OFETs printed onto other biodegradable materials. Small device-to-device variation was achieved on a set of 8 devices, with limited I_{DS} standard deviations (of 25 % and 13 % in linear and saturation regimes, respectively) and limited mobility standard deviations (of 15 % and 13 % in linear and saturation regimes, respectively). The proper operation of the devices was also demonstrated through electrical characterization performed after delamination and rolling with a bending radius of 2.5 mm.

The biochemical oxygen demand test highlighted a slightly slower but still satisfactory degradation rate for the OFETs printed onto PHB substrate compared to the pristine PHB film. Interestingly, these results are consistent with similar devices printed on other biopolymers.

In conclusion, PHB has proven to be compatible with the fabrication of large-area, all-organic electronics, and offers a promising path for future electronic devices in biomedical and food packaging applications, where mechanical flexibility, good electrical performance, small device-to-device variation and cost-effective fabrication with a low carbon footprint are mandatory, and biodegradability would be an additional value.

CRediT authorship contribution statement

Fabrizio A. Viola: Writing – original draft, Methodology, Investigation, Formal analysis, Conceptualization. **Ksenija Maksimovic:** Writing – original draft, Methodology, Investigation, Data curation. **Pietro Cataldi:** Writing – review & editing, Methodology, Investigation, Data curation. **Camilla Rinaldi:** Methodology, Investigation. **Elena Stucchi:** Methodology, Investigation. **Filippo Melloni:** Methodology. **Athanassia Athanassiou:** Supervision, Resources. **Mario Caironi:** Writing – review & editing, Supervision, Resources, Funding acquisition, Conceptualization.

Declaration of competing interest

The authors declare that they have no known competing financial interests or personal relationships that could have appeared to influence the work reported in this paper.

Data availability

Data will be made available on request.

Acknowledgements

MC acknowledges the financial support of the European Research Council (ERC) under the European Union's Horizon 2020 research and innovation program "ELFO", Grant Agreement 864299.

FAV acknowledges the financial support of The Italian Ministry of Universities and Research (MUR) - Young Researchers SoE Grant: SOE_0000104 (wEAR Project).

This work is part of the Flagship for Sustainable Technologies programme of Istituto Italiano di Tecnologia.

Appendix A. Supplementary data

Supplementary data to this article can be found online at https://doi.org/10.1016/j.mtbio.2024.101274.

References

[1] O.S. Shittu, I.D. Williams, P.J. Shaw, Global E-waste management: can WEEE make a difference? A review of e-waste trends, legislation, contemporary issues and future challenges, Waste Manag. 120 (2021) 549–563, https://doi.org/10.1016/j.wasman.2020.10.016.

[2] C.P. Baldé, R. Kuehr, T. Yamamoto, R. McDonald, E. D'Angelo, S. Althaf, G. Bel, O. Deubzer, E. Fernandez-Cubillo, V. Gray, S. Herat, S. Honda, G. Iattoni, D. S. Khetriwal, V.L. di Cortemiglia, Y. Lobuntsova, I. Nnorom, N. Pralat, M. Wagner, Global E-waste Monitor 2024 (2024) 10–17. https://ewastemonitor.info/the-global-e-waste-monitor-2024/.

[3] K. Liu, Q. Tan, J. Yu, M. Wang, A global perspective on e-waste recycling, Circ. Econ. 2 (2023) 100028, https://doi.org/10.1016/j.cec.2023.100028.

[4] S. Chandrasekaran, A. Jayakumar, R. Velu, A comprehensive review on printed electronics: a technology drift towards a sustainable future, Nanomaterials 12 (2022), https://doi.org/10.3390/nano12234251.

[5] Y. Xie, C. Ding, Q. Jin, L. Zheng, Y. Xu, H. Xiao, M. Cheng, Y. Zhang, G. Yang, M. Li, L. Li, M. Liu, Organic transistor-based integrated circuits for future smart life, SmartMat. n/a (2024) e1261, https://doi.org/10.1002/smm2.1261.

[6] Y. Bonnassieux, C.J. Brabec, Y. Cao, T.B. Carmichael, M.L. Chabinyc, K.-T. Cheng, G. Cho, A. Chung, C.L. Cobb, A. Distler, H.-J. Egelhaaf, G. Grau, X. Guo, G. Haghiashtiani, T.-C. Huang, M.M. Hussain, B. Iniguez, T.-M. Lee, L. Li, Y. Ma, D. Ma, M.C. McAlpine, T.N. Ng, R. Österbacka, S.N. Patel, J. Peng, H. Peng, J. Rivnay, L. Shao, D. Steingart, R.A. Street, V. Subramanian, L. Torsi, Y. Wu, The 2021 flexible and printed electronics roadmap, Flex. Print. Electron. 6 (2021) 23001, https://doi.org/10.1088/2058-8585/abf986.

[7] C.S. Buga, J.C. Viana, A review on materials and technologies for organic large-area electronics, Adv. Mater. Technol. 6 (2021) 2001016, https://doi.org/10.1002/admt.202001016.

[8] F.A. Viola, F. Melloni, A. Molazemhosseini, F. Modena, M. Sassi, L. Beverina, M. Caironi, A n-type, stable electrolyte gated organic transistor based on a printed polymer, Adv. Electron. Mater. (2022) 2200573, https://doi.org/10.1002/aelm.202200573.

[9] P. Zhao, X. Wang, Y. Tong, X. Zhao, Q. Tang, Y. Liu, Transfer-printing of insoluble conducting polymer for soft 3D conformal all-organic transistors, Small. n/a (2024) 2309263, https://doi.org/10.1002/smll.202309263.

[10] W. Li, Q. Liu, Y. Zhang, A. Li, Z. He, W.C. H Choy, P.J. Low, P. Sonar, A. Ko Ko Kyaw, W. Li, Y. Zhang, C. Li, Z. He, A.K. K Kyaw, Q. Liu, P. Sonar, W.C. H Choy, Biodegradable materials and green processing for green electronics, Adv. Mater. 32 (2020), https://doi.org/10.1002/adma.202001591.

[11] G. Casula, S. Lai, L. Matino, F. Santoro, A. Bonfiglio, P. Cosseddu, Printed, low-voltage, all-organic transistors and complementary circuits on paper substrate, Adv. Electron. Mater. 6 (2020) 1901027, https://doi.org/10.1002/aelm.201901027.

[12] D. Zhao, Y. Zhu, W. Cheng, W. Chen, Y. Wu, H. Yu, Cellulose-based flexible functional materials for emerging intelligent electronics, Adv. Mater. 33 (2021) 2000619, https://doi.org/10.1002/adma.202000619.

[13] Z. Rafiee, A. Elhadad, S. Choi, Revolutionizing papertronics: advanced green, tunable, and flexible components and circuits, Adv. Sustain. Syst. n/a (2024) 2400049, https://doi.org/10.1002/adsu.202400049.

[14] T. Xing, A. He, Z. Huang, Y. Luo, Y. Zhang, M. Wang, Z. Shi, G. Ke, J. Bai, S. Zhao, F. Chen, W. Xu, Silk-based flexible electronics and smart wearable Textiles: progress and beyond, Chem. Eng. J. 474 (2023) 145534, https://doi.org/10.1016/j.cej.2023.145534.

[15] J.W. Chae, D. Lee, A. Osman, B. Kang, J. Hwang, W. Kim, D. Kim, W.H. Lee, S. M. Won, Silk fibroin, sericin, and conductive silk composites for skin-attachable transient electronics, ACS Appl. Electron. Mater. 6 (2024) 1746–1756, https://doi.org/10.1021/acsaelm.3c01663.

[16] C. Lu, X. Wang, X.Y. Liu, Flexible meso electronics and photonics based on cocoon silk and applications, ACS Biomater. Sci. Eng. (2024), https://doi.org/10.1021/acsbiomaterials.4c00254.
[17] N. Thombare, S. Kumar, U. Kumari, P. Sakare, R.K. Yogi, N. Prasad, K.K. Sharma, Shellac as a multifunctional biopolymer: a review on properties, applications and future potential, Int. J. Biol. Macromol. 215 (2022) 203–223, https://doi.org/10.1016/j.ijbiomac.2022.06.090.
[18] R.N. Hussein, K. Schlingman, C. Noade, R.S. Carmichael, T.B. Carmichael, Shellac-paper composite as a green substrate for printed electronics, Flex. Print. Electron. 7 (2022) 45007, https://doi.org/10.1088/2058-8585/ac9f54.
[19] D. Skaf, T.C. Gomes, R. Majidzadeh, R.N. Hussein, T.B. Carmichael, S. Rondeau-Gagné, Shellac as dielectric materials in organic field-effect transistors: from silicon to paper substrates, Flex. Print. Electron. 8 (2023) 24002, https://doi.org/10.1088/2058-8585/acda48.
[20] G. Balakrishnan, A. Bhat, D. Naik, J.S. Kim, S. Marukyan, L. Gido, M. Ritter, A. S. Khair, C.J. Bettinger, Gelatin-based ingestible impedance sensor to evaluate gastrointestinal epithelial barriers, Adv. Mater. 35 (2023) 2211581, https://doi.org/10.1002/adma.202211581.
[21] S. Moreno, J. Keshtkar, R.A. Rodriguez-Davila, A. Bazaid, H. Ibrahim, B. J. Rodriguez, M.A. Quevedo-Lopez, M. Minary-Jolandan, Bioelectronics on mammalian collagen, Adv. Electron. Mater. 6 (2020) 2000391, https://doi.org/10.1002/aelm.202000391.
[22] M.M.O. Netto, W.B. Gonçalves, R.W.C. Li, J. Gruber, Biopolymer based ionogels as active layers in low-cost gas sensors for electronic noses, Sensors Actuators B Chem. 315 (2020) 128025, https://doi.org/10.1016/j.snb.2020.128025.
[23] X. Peng, K. Dong, Y. Zhang, L. Wang, C. Wei, T. Lv, Z.L. Wang, Z. Wu, Sweat-permeable, biodegradable, transparent and self-powered chitosan-based electronic skin with ultrathin elastic gold nanofibers, Adv. Funct. Mater. 32 (2022) 2112241, https://doi.org/10.1002/adfm.202112241.
[24] Y. Wang, L. Wang, Y. Lu, Q. Zhang, Y. Fang, D. Xu, J. Cai, Stretchable, biodegradable dual cross-linked chitin hydrogels with high strength and toughness and their potential applications in flexible electronics, ACS Sustain. Chem. Eng. 11 (2023) 7083–7093, https://doi.org/10.1021/acssuschemeng.3c00184.
[25] M. Mangal, C.V. Rao, T. Banerjee, Bioplastic: an eco-friendly alternative to non-biodegradable plastic, Polym. Int. 72 (2023) 984–996, https://doi.org/10.1002/pi.6555.
[26] K. Chauhan, R. Kaur, I. Chauhan, Sustainable bioplastic: a comprehensive review on sources, methods, advantages, and applications of bioplastics, Polym. Technol. Mater. 63 (2024) 913–938, https://doi.org/10.1080/25740881.2024.2307369.
[27] É. Bozó, H. Ervasti, N. Halonen, S.H.H. Shokouh, J. Tolvanen, O. Pitkänen, T. Järvinen, P.S. Pálvölgyi, Á. Szamosvölgyi, A. Sápi, Z. Konya, M. Zaccone, L. Montalbano, L. De Brauwer, R. Nair, V. Martínez-Nogués, L. San Vicente Laurent, T. Dietrich, L. Fernández de Castro, K. Kordas, Bioplastics and carbon-based sustainable materials, components, and devices: toward green electronics, ACS Appl. Mater. Interfaces 13 (2021) 49301–49312, https://doi.org/10.1021/acsami.1c13787.
[28] A.I. Barzic, An introduction to engineering applications of bioplastics, in: Handb. Bioplastics Biocomposites Eng. Appl, 2023, pp. 1–22, https://doi.org/10.1002/9781119160182.ch1.
[29] X. Hou, S. Liu, C. He, Designing ultratough, malleable and foldable biocomposites for robust green electronic devices, J. Mater. Chem. A. 10 (2022) 1497–1505, https://doi.org/10.1039/d1ta09128j.
[30] E. Luoma, M. Välimäki, J. Ollila, K. Heikkinen, K. Immonen, Bio-based polymeric substrates for printed hybrid electronics, Polymers 14 (2022), https://doi.org/10.3390/polym14091863.
[31] W. Peng, L. Wang, M. Zhang, D.-G. Yu, X. Li, Biodegradable flexible conductive film based on sliver nanowires and PLA electrospun fibers, J. Appl. Polym. Sci. 141 (2024) e55433, https://doi.org/10.1002/app.55433.
[32] V. Sharma, R. Sehgal, R. Gupta, Polyhydroxyalkanoate (PHA): properties and modifications, Polymer (Guildf) 212 (2021) 123161, https://doi.org/10.1016/j.polymer.2020.123161.
[33] G. Gorrasi, R. Pantani, Effect of PLA grades and morphologies on hydrolytic degradation at composting temperature: assessment of structural modification and kinetic parameters, Polym. Degrad. Stab. 98 (2013) 1006–1014, https://doi.org/10.1016/j.polymdegradstab.2013.02.005.
[34] Roohi, M.R. Zaheer, M. Kuddus, PHB (poly-β-hydroxybutyrate) and its enzymatic degradation, Polym. Adv. Technol. 29 (2018) 30–40, https://doi.org/10.1002/pat.4126.
[35] P. Cataldi, P. Steiner, T. Raine, K. Lin, C. Kocabas, R.J. Young, M. Bissett, I. A. Kinloch, D.G. Papageorgiou, Multifunctional biocomposites based on polyhydroxyalkanoate and graphene/carbon nanofiber hybrids for electrical and thermal applications, ACS Appl. Polym. Mater. 2 (2020) 3525–3534, https://doi.org/10.1021/acsapm.0c00539.
[36] B. McAdam, M. Brennan Fournet, P. McDonald, M. Mojicevic, Production of polyhydroxybutyrate (PHB) and factors impacting its chemical and mechanical characteristics, Polymers 12 (2020), https://doi.org/10.3390/polym12122908.
[37] O. Olejnik, A. Masek, J. Zawadziłło, Processability and mechanical properties of thermoplastic polylactide/polyhydroxybutyrate (PLA/PHB) bioblends, Materials 14 (2021), https://doi.org/10.3390/ma14040898.
[38] E. Stucchi, K. Maksimovic, L. Bertolacci, F.A. Viola, A. Athanassiou, M. Caironi, Biodegradable all-polymer field-effect transistors printed on Mater-Bi, J. Inf. Disp. 22 (2021) 247–256, https://doi.org/10.1080/15980316.2021.1990145.
[39] P. Anbukarasu, D. Sauvageau, A. Elias, Tuning the properties of polyhydroxybutyrate films using acetic acid via solvent casting, Sci. Rep. 5 (2016).
[40] D. Prat, J. Hayler, A. Wells, A survey of solvent selection guides, Green Chem. 16 (2014) 4546–4551, https://doi.org/10.1039/c4gc01149j.
[41] D. Natali, M. Caironi, Charge injection in solution-processed organic field-effect transistors: physics, models and characterization methods, Adv. Mater. 24 (2012) 1357–1387, https://doi.org/10.1002/adma.201104206.
[42] Y. Zhou, C. Fuentes-Hernandez, J. Shim, J. Meyer, A. Giordano, H. Li, P. Winglet, T. Papadopoulos, H. Cheun, J. Kim, M. Fenoll, A. Dindar, W. Haske, E. Jafabadi, T. Khan, H. Sojoudi, S. Barlow, S. Graham, J. Bredas, S. Marder, A. Kahn, B. Kippelen, A universal method to produce low–work function electrodes for organic electronics, Science (2012) 336, https://doi.org/10.1126/science.1219274.
[43] E. Stucchi, A.D. Scaccabarozzi, F.A. Viola, M. Caironi, Ultraflexible all-organic complementary transistors and inverters based on printed polymers, J. Mater. Chem. C 8 (2020) 15331–15338, https://doi.org/10.1039/D0TC03064C.
[44] F.A. Viola, B. Brigante, P. Colpani, G. Dell'Erba, V. Mattoli, D. Natali, M. Caironi, A 13.56 MHz rectifier based on fully inkjet printed organic diodes, Adv. Mater. 32 (2020) 1–7, https://doi.org/10.1002/adma.202002329.
[45] G.B. Blanchet, C.R. Fincher, M. Lefenfeld, J.A. Rogers, Contact resistance in organic thin film transistors, Appl. Phys. Lett. 84 (2004) 296–298, https://doi.org/10.1063/1.1639937.
[46] D. Natali, L. Fumagalli, M. Sampietro, Modeling of organic thin film transistors: effect of contact resistances, J. Appl. Phys. 101 (2007), https://doi.org/10.1063/1.2402349.
[47] H. Klauk, Organic Electronics: Materials, Manufacturing, and Applications, 2006.
[48] H.H. Choi, K. Cho, C.D. Frisbie, H. Sirringhaus, V. Podzorov, Critical assessment of charge mobility extraction in FETs, Nat. Mater. 17 (2017) 2–7, https://doi.org/10.1038/nmat5035.
[49] E.Y. Shin, E.Y. Choi, Y.Y. Noh, Parylene based bilayer flexible gate dielectric layer for top-gated organic field-effect transistors, Org. Electron. 46 (2017) 14–21, https://doi.org/10.1016/j.orgel.2017.04.005.
[50] T. Sekitani, S. Iba, Y. Kato, Y. Noguchi, T. Someya, T. Sakurai, Ultraflexible organic field-effect transistors embedded at a neutral strain position, Appl. Phys. Lett. 87 (2005) 173502, https://doi.org/10.1063/1.2115075.
[51] A. Chamas, H. Moon, J. Zheng, Y. Qiu, T. Tabassum, J.H. Jang, M. Abu-Omar, S. L. Scott, S. Suh, Degradation rates of plastics in the environment, ACS Sustain. Chem. Eng. 8 (2020) 3494–3511, https://doi.org/10.1021/acssuschemeng.9b06635.
[52] A.R. Bagheri, C. Laforsch, A. Greiner, S. Agarwal, Fate of so-called biodegradable polymers in seawater and freshwater, Glob. Challenges. 1 (2017) 1700048, https://doi.org/10.1002/gch2.201700048.